

Four-level polarization discriminator based on a surface plasmon polaritonic crystal

M. I. Benetou,^{1,a)} B. C. Thomsen,¹ P. Bayvel,¹ W. Dickson,² and A. V. Zayats²

¹*Optical Networks Group, Department of Electronic and Electrical Engineering, University College London, London WC1E 7JE, United Kingdom*

²*Nano-optics and Near-field Spectroscopy Group, Department of Physics, King's College London, Strand, London WC2R 2LS, United Kingdom*

(Received 21 December 2010; accepted 3 February 2011; published online 17 March 2011)

A compact, four-level polarization discriminator based on a surface plasmon polaritonic crystal (SPPC) has been experimentally demonstrated. It is able to uniquely resolve and spatially separate four signals that have been linearly polarized at azimuth angles 0°, 45°, 90°, and 135°. It exploits the excitation of multiple surface plasmon polariton eigenmodes in nondegenerate directions when the SPPC is illuminated with monochromatic light. The device is planar and of micrometer scale, which makes it suitable for on-chip integration and miniaturization of photonic circuits. © 2011 American Institute of Physics. [doi:10.1063/1.3561748]

In optical communications and signal processing, polarization of a carrier wave is an additional degree of freedom that can be used for information management. For example, multiplexing signal in two orthogonal polarization states doubles the bandwidth of the system.¹ Alternatively, one can use polarization shift-keying for encoding digital signal in different polarization states of a carrier wave.² At the same time, the integration and the reduction in the photonic circuit size is essential if photonics is to see widespread deployment for applications in short range interconnects and optical signal processing. In this context, plasmonics provides unprecedented opportunity in the development of subwavelength waveguide circuitry and miniaturization of photonic components for light manipulation.^{3–6} Since surface plasmon polaritons (SPPs), which are surface waves resulting from the efficient coupling between photons and free electron oscillations on a metal-dielectric interface, are intrinsically TM-polarized,³ they are very attractive for polarization management.⁴ SPPs preserve their polarization state during propagation and, in turn, their propagation direction can be controlled with the polarization of the excitation light. The excitation of the SPP waves is a highly broadband effect ranging from ultraviolet to infrared.⁵

This letter experimentally demonstrates a four-level polarization discriminator at telecommunication wavelengths, which is based on a two-dimensional surface plasmon polaritonic crystal (SPPC)—a periodically structured metal-dielectric film. It is able to uniquely resolve and spatially separate four linearly polarized states with azimuth angles $\theta=0^\circ, 45^\circ, 90^\circ,$ and 135° . The device is planar and circular with a 40 μm diameter, which makes it easy to combine with other plasmonic or planar dielectric components in integrated photonic chips.

A scanning electron microscopy (SEM) image of the SPPC used in the experiments is shown in Fig. 1(a). The structure was fabricated by focused-ion beam milling in a magnetron-sputtered Au film. It is formed by 300 nm diameter holes, periodically perforated in a square lattice with a 1500 nm period, in 50 nm thick gold film, deposited on a

glass substrate. The period of the lattice determines the wavelength range in which the device operates.⁷ The SPPC was surrounded by a 120 μm diameter circular slit milled in the gold film, as shown in Fig. 1(b), to allow the signal carried by SPPs to be detected in the far field after scattering into photons. The SPPC transmission dispersion was investigated by measuring the zero-order far-field transmission spectra of the crystal for different angles of incidence under illumination with polarized collimated light, as described, e.g., in Ref. 8.

An SPPC with a square lattice supports several SPP Bloch modes that are the eigenmodes of the structure,⁵ so that

$$\vec{k}_{\text{BSPP}} = \vec{k}_{\text{SPP}} + \frac{2\pi}{D}(p\vec{u}_x + q\vec{u}_y), \quad (1)$$

where \vec{k}_{BSPP} and \vec{k}_{SPP} are the wave vectors of the SPP Bloch modes on the crystal and the SPPs on a smooth surface, respectively, D is the lattice period, \vec{u}_x and \vec{u}_y are the unit vectors of the reciprocal lattice, and p and q are integers. These modes can be identified in the dispersion of the transmission through the SPPC since they are responsible for the transmission enhancement.⁹

Figure 1(c) shows the dispersion of the transmission through the SPPC sample when illuminated with horizontally polarized infrared light. The band gaps are denoted as the dark regions, while the SPP eigenmodes, denoted by the labeled arrows, lie in their vicinity;⁷ the solid lines show the approximately estimated eigenmodes using Eq. (1). As it can be seen, the SPPC has been designed such that the (1,0) and (0,1) SPP Bloch modes of the air-Au interface are spectrally situated close to the $(\pm 1,1)$ modes of the glass-Au interface, in the center of the Brillouin zone. The (0,1) eigenmode replaces the (1,0) one under the orthogonally polarized illumination. When the SPPC is illuminated with a 7° divergent beam, corresponding spectral region is highlighted in Fig. 1(c), four Bloch modes can be excited at the same time: two in Γ -X direction at the air-Au interface and two in Γ -M direction at the glass-Au interface.

In order to investigate the simultaneous excitation of the four different eigenmodes and its effect on the polarization

^{a)}Electronic mail: m.benetou@ee.ucl.ac.uk.

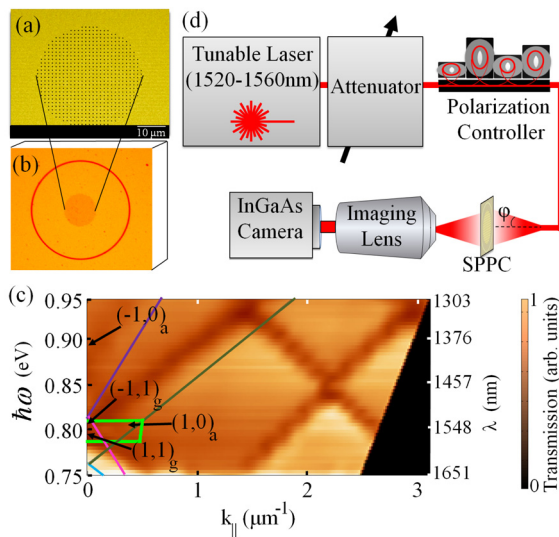


FIG. 1. (Color online) (a) SEM image of the SPPC and (b) optical microscope image of the SPPC surrounded by a scattering ring. (c) Measured SPPC transmission dispersion (2D map) and (lines) eigenmode positions estimated from Eq. (1); notations “a” and “g” correspond to the modes of air-Au and glass-Au interfaces, respectively. (d) Experimental arrangement for characterization of the SPPC wavelength and polarization dispersive properties.

dispersion properties of the SPPC, the experimental arrangement shown in Fig. 1(d) was used. The SPPC was illuminated through an antireflection-coated single-mode fiber coupled to a polarization controller and a tunable infrared laser. The SPPC was positioned approximately $80 \mu\text{m}$ from the fiber end; this fiber-sample separation was selected in order to illuminate the SPPC but not the surrounding scattering ring. The fiber numerical aperture was 0.13, such that the SPPC was illuminated in the range of 0° – 7° angles of incidence and the excitation of the four eigenmodes was enabled. The illuminating light polarization was controlled by the polarization controller. The transmitted light was collected by an antireflection coated imaging lens ($\times 10$, $\text{NA} = 0.17$) and detected by the InGaAs camera, such as the far field intensity distribution of the SPP waves scattered by the ring was imaged.

Figure 2 shows the intensity distribution on and around the SPPC under the illumination with linearly polarized light at azimuth angles $\theta = 0^\circ, 45^\circ, 90^\circ$, and 135° . The central area is the image of the SPPC itself and is saturated due to the high direct transmission through the crystal. The SPP waves observed at the spatially separated angles of $\alpha = 0^\circ, 45^\circ, 90^\circ$, and 135° correspond to the SPP eigenmodes discussed above; SPP waves corresponding to the same eigenmodes are observed in the counterpart hemisphere. The observed SPP waves are launched by the crystal on the surrounding smooth Au film and observed into the far field after being converted into photons by the scattering ring. To quantitatively analyze the captured images, these were first transformed into polar coordinates and then the optical power was integrated over an annular aperture that encompasses the scattering ring. The SPP power detected at the different angles around the SPPC depends both on the wavelength and the orientation of the polarization of the incident light with respect to the crystal axes. Due to the longitudinal nature of the SPP waves, the coupling efficiency to one eigenmode for a given wavelength is maximized when the electric field orientation of the inci-

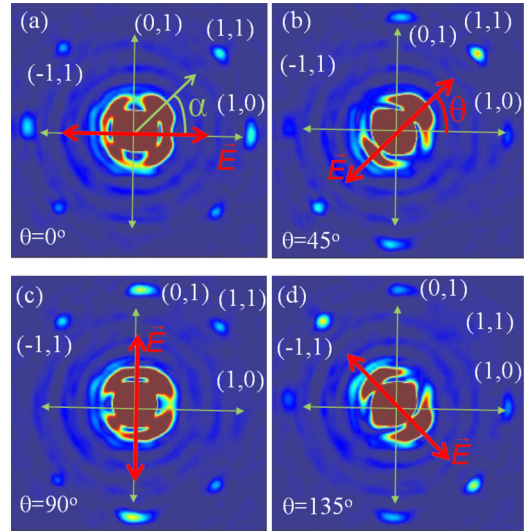


FIG. 2. (Color online) Far-field intensity distributions measured for the SPPC in Fig. 1(a) when illuminated with linearly polarized light with $\lambda = 1539 \text{ nm}$ and azimuth angles θ equal to (a) 0° , (b) 45° , (c) 90° , and (d) 135° .

dent light on the crystal coincides with the eigenmode orientation ($\alpha = \theta$ and $\theta + \pi$).^{5,10} The wavelength dependence of the SPP detected power is a combination of the wavelength-dependent coupling efficiency to the several excited eigenmodes and the propagation of the eigenmodes on interfaces with unequal refractive indices, air-Au interface and glass-Au interface.

To investigate the wavelength dependence of the coupling efficiency combined with the propagation losses experienced by the four eigenmodes, the illuminating light polarization state was set to be linear with azimuth angles $\theta = 0^\circ, 45^\circ, 90^\circ$, and 135° and its wavelength was varied from 1520 to 1560 nm with 1 nm step, for each of the polarization states. Figure 3(a) shows the SPP transmission power integrated over $\Delta\alpha = \pm 15^\circ$ angular range around the four principal angles $\alpha = 0^\circ, 45^\circ, 90^\circ$, and 135° of the scattering ring corresponding to the excited eigenmodes (1,0), (1,1), (0,1), and (-1,1), respectively, as a function of the illuminating wavelength. Since the eigenmodes propagate symmetrically with respect to the center of the crystal, the detected power around angles with a 180° difference were added together to eliminate any power fluctuations due to misalignment between the fiber and the sample. The four eigenmodes were plotted for the case that the polarization state of the illuminating light was that required to maximize the coupling efficiency. For a polarization discriminator, the polarization states to be detected should have similar powers. As can be seen, there is a 7 nm range around the operating wavelength of 1539 nm over which there is less than 1 dB variation in the power around the four principal angles of the crystal; this range is defined in Fig. 3(a) as “1 dB colorless bandwidth.”

The polarization dispersion properties of the device were characterized at its operating wavelength. The polarization state of the illuminating light was set to be linear with azimuth angle θ varied from 0° to 360° with a 5° step. Figure 3(b) shows the signal measured from the device around the principal angles corresponding to the excited eigenmodes, as a function of the incident polarization azimuth angle θ . It can be observed that signals polarized at azimuth angles $\theta = 0^\circ, 45^\circ, 90^\circ$, and 135° can be uniquely analyzed with 6 dB ex-

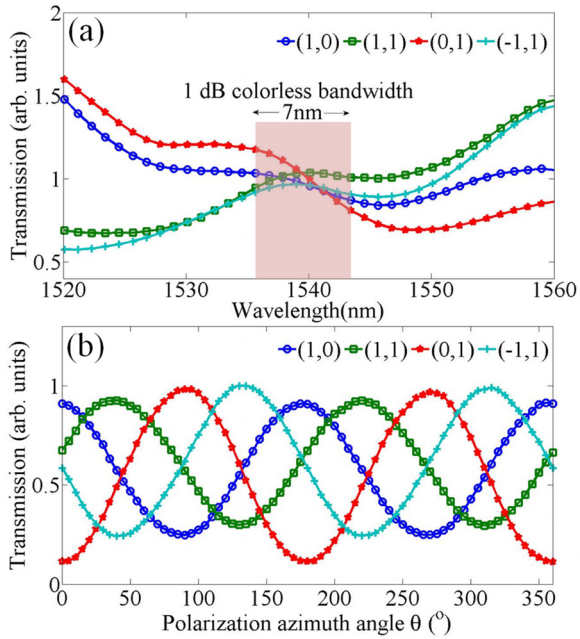


FIG. 3. (Color online) (a) Wavelength and (b) polarization dependences of the SPP signal transmission at the angular positions corresponding to the excited eigenmodes, measured at the scattering ring around the crystal.

tion ratio and spatially separated at corresponding angles around the SPPC.

In conclusion, a four-level polarization discriminator based on a SPPC able to uniquely spatially resolve signals linearly polarized at four different azimuth angles has been experimentally demonstrated. The device is planar, micrometer scale, and easily integrable. It offers a 7 nm (at 1 dB)

colorless-bandwidth and its operating wavelength can be tuned, by changing the parameters of the crystal, across the hole spacing of the sample across the whole spectra range from ultraviolet to infrared whole spectra range. Such multi-level polarization sensitive elements can be used to miniaturize the receiver for multilevel polarization shift-keying systems or for systems which combine polarization and wavelength multiplexing/shift-keying, to further increase the throughput in short-distance transmission networks. Finally it is ideal for integration with other nanophotonic elements with the aim of miniaturization of photonic circuits.

This work was supported in part by the EPSRC (UK) and the Royal Society (UK).

¹A. Gnauck, G. Charlet, P. Tran, P. Winzer, C. Doerr, J. Centanni, E. Burrows, T. Kawanishi, T. Sakamoto, and K. Higuma, *J. Lightwave Technol.* **26**, 79 (2008); N. Chi, S. Yu, L. Xu, and P. Jeppesen, *Electron. Lett.* **41**, 547 (2005).

²M. Nazarathy and E. Simony, *J. Lightwave Technol.* **24**, 1978 (2006).

³H. Raether, *Surface Plasmons* (Springer, Berlin, 1988).

⁴E. Laux, C. Genet, T. Skauli, and T. W. Ebbesen, *Nat. Photonics* **2**, 161 (2008).

⁵A. V. Zayats, I. I. Smolyaninov, and A. A. Maradudin, *Phys. Rep.* **408**, 131 (2005).

⁶N.-N. Feng, M. Brongersma, and L. dal Negro, *IEEE J. Quantum Electron.* **43**, 479 (2007).

⁷W. L. Barnes, T. W. Preist, S. C. Kitson, and J. R. Sambles, *Phys. Rev. B* **54**, 6227 (1996).

⁸W. Dickson, G. A. Wurtz, P. R. Evans, R. J. Pollard, and A. V. Zayats, *Nano Lett.* **8**, 281 (2008).

⁹A. V. Zayats, L. Salomon, and F. D. Fornel, *J. Microsc.* **210**, 344 (2003); L. Salomon, F. Grillot, A. V. Zayats, and F. de Fornel, *Phys. Rev. Lett.* **86**, 1110 (2001).

¹⁰V. Mikhailov, G. A. Wurtz, J. Elliott, P. Bayvel, and A. V. Zayats, *Phys. Rev. Lett.* **99**, 083901 (2007).